Direct Observation of Ultrafast Electron Injection from Coumarin 343 to TiO_2 Nanoparticles by Femtosecond Infrared Spectroscopy

Hirendra N. Ghosh, John B. Asbury, and Tianquan Lian*

Department of Chemistry, Emory University, Atlanta, Georgia 30322

Received: April 9, 1998; In Final Form: June 22, 1998

Transient infrared (IR) absorption of injected electrons in colloidal TiO_2 nanoparticles in the 1900−2000 cm^{-1} region are measured by femtosecond IR spectroscopy. The direct detection of electrons in the nanoparticles with subpicosecond time resolution provides a new approach to study ultrafast interfacial electron transfer between semiconductor nanoparticles and molecular adsorbates. The dynamics of electron injection from sensitizers to nanoparticles and the subsequent back-transfer and relaxation dynamics of the injected electrons correspond to the rise and decay of the transient IR signal of injected electrons. Using this technique, the injection time for coumarin 343 sensitized TiO_2 nanoparticles in D_2O is determined to be 125 ± 25 fs. The subsequent decay dynamics of the injected electrons in nanoparticles are found to be different from conduction band electrons in a bulk TiO_2 crystal.

Introduction

Interfacial electron transfer (ET) between molecular adsorbates and semiconductors has been a subject of intense current research interests.[1−3] The understanding of this fundamental process is essential for the application of many semiconductor devices, such as photoelectrochemical solar cells that are based on dye sensitized nanocrystalline TiO_2 thin films.[4] Unlike in homogeneous solutions,[5−7] ET dynamics in the solid−liquid interface[8−11] are still poorly understood.[1,2,12] The interfacial nature of these processes has hindered the theoretical and experimental studies in the past. Most of the previous understanding of bulk semiconductor−liquid interfacial charge transfer is derived indirectly from steady-state photocurrent measurements in electrochemical cells.[1,12,13] Unfortunately, obtaining ET rates from steady-state photocurrent is often quite complicated because the latter depends on many other interface and bulk properties in addition to the interfacial ET rates.[1,12] On the other hand, studies of adsorbates on semiconductor or metal surfaces in UHV chambers[14] have gained great insights into small molecule/solid interaction, but they may be oversimplified models for the solid−liquid interface. Efforts in developing in situ, direct, and interface specific spectroscopic techniques have resulted in some elegant yet complicated techniques, such as sum frequency (SFG) and second harmonic (SHG) generation[15−17] and the surface restricted grating technique.[18]

In recent years, electron transfer between semiconductor nanoparticles and dye sensitizers has been intensely studied by ultrafast laser spectroscopy.[18−33] By measuring the excited-state dynamics of the sensitizer through transient absorption or fluorescence decay, the electron injection rates from various adsorbed dye molecules into various semiconductor nanoparticles have been inferred, ranging from subpicoseconds[20,25−27] to tens of picoseconds[34] and even nanoseconds.[35] Most transient absorption studies in the visible and near-IR region are hindered by spectral overlap of absorptions in various electronic states, such as the excited states, cationic state, and ground state, as well as stimulated emission. Fluorescence quenching studies are often complicated by non-ET-related quenching pathways, such as energy transfer among sensitizer molecules[22,28] and the dynamic fluorescence Stokes shift.[33] Because of these complexities, there have been many conflicting reports of electron-transfer rates,[20,25] and a systematic study of the dependence of interfacial ET rates on various adsorbate/nanoparticle properties has not been achieved. In addition, in most earlier studies, except for three recent reports,[19−21] only the dye molecules are monitored; hence, the nature and dynamics of the injected electrons remain unknown.

To systematically study ET dynamics in the solid−liquid interface, new in situ techniques that are capable of assigning the ET process unambiguously and that complement the existing visible/near-IR transient absorption and fluorescence quenching techniques are needed. Femtosecond mid-IR spectroscopy[36] provides such an approach for these interfacial problems because it can directly study the dynamics of electrons in the semiconductor in addition to adsorbates. As demonstrated in bulk[37,38] and quantum well[39] semiconductor materials, valence band holes and conduction band electrons in semiconductors have strong absorptions in the infrared region. These absorptions consist of free carrier absorption,[40] which is often broad and increases with wavelength, intraband transitions[40] between different valleys (or subbands) within the conduction or the valence bands, and absorptions of trap states. Since these IR absorptions of electrons are direct evidence for the arrival of electrons inside semiconductors, they provide an unambiguous spectroscopic probe for studying interfacial electron transfer between semiconductor and adsorbates. Furthermore, unlike fluorescence quenching, femtosecond IR spectroscopy is a general technique. It can be used for any adsorbate/nanoparticle systems, allowing a systematic study of the dependence of ET rates on the properties of the adsorbates, semiconductors, and the solvent environments.

In two recent studies of electron injection in Ru(II)(2,2′-bipyridyl-4,4′-dicarboxylate)$_2$(NCS)$_2$ (Ru N3 dye) sensitized TiO_2 thin films, transient near-IR absorption signals at 1.1[20] and 1.5 μm[21] were attributed to injected electrons in TiO_2. Since

* To whom correspondence should be addressed. e-mail tlian@emory.edu, fax (404) 727-6586, phone (404) 727-6649.

S1089-5647(98)01806-9 CCC: $15.00
Published on Web 07/30/1998

the near-IR absorption cross section for electrons in semiconductor is often smaller than that in the mid- to far-IR[40] and these signals may be complicated by absorptions of the sensitizer excited states in the near-IR,[47b] it is more desirable to probe the electrons at longer wavelengths. As demonstrated in $[Ru(II)(dceb)(bpy)_2]^{2+}$ sensitized nanocrystalline TiO_2 thin films, a broad mid-IR absorption signal was observed to appear with a <30 ps instrument response limited rise time and attributed to injected electrons.[19] In this paper, we describe our recent study of electron injection from adsorbed coumarin 343 (C-343) dye to TiO_2 nanoparticles using subpicosecond infrared spectroscopy in the mid-IR region. This study is focused on the characterization of the IR absorption of injected electrons in colloidal nanoparticles, as well as the demonstration of studying interfacial ET using this spectral signature of electrons with subpicosecond time resolution. C-343 sensitized TiO_2 nanoparticles are chosen for this study because (a) this system is known to undergo efficient electron injection[26,41] and (b) C-343 molecules have no noticeable absorptions in the 5 μm region (see below), which facilitates the assignment of IR absorption of injected electrons.

Experimental Section

Femtosecond IR Spectrometer. The femtosecond infrared spectrometer used for this study is based on an amplified femtosecond Ti:sapphire laser system from Clark-MXR (1 kHz repetition rate at 800 nm, 100 fs, 900 μJ/pulse) and nonlinear frequency mixing techniques. Briefly, the 800 nm output pulse from the regenerative amplifier is split into two parts. One part, with about 600 μJ/pulse, is used to pump a Clark IR OPA (optical parametric amplifier) to generate two tunable near-IR pulses from 1.1 to 2.5 μm. These signal and idler pulses are combined in a $AgGaS_2$ crystal to generate mid-IR pulses from 3 to 10 μm by difference frequency generation. The mid-IR pulses, with pulse energy of about 1 μJ, have a typical intensity fluctuation of about 1−3%. The other part of the 800 nm pulse, with 300 μJ/pulse, is used to generate pump pulses. Currently using second harmonic generation (SHG) and third harmonic generation (THG) in BBO crystals, UV pulses at 400 nm with pulse energy of about 40 μJ and at 266 nm with about 5 μJ are generated. The femtosecond IR spectrometer has a typical time resolution of about 150−200 fs (fwhm) for an UV pump, mid-IR probe experiment.

The probe IR pulses are divided into a signal and a reference beam. While the signal beam measures the absorption of the sample, the reference beam is used to normalize the laser intensity fluctuation. Both beams are then dispersed in a monochromator. A 2−3 cm^{-1} slice of the total spectrum (approximately 200 cm^{-1}) is measured by a pair of HgCdTe detectors for each laser pulse. Transient absorption spectra are recorded by scanning the monochromator. The typical short-term noise level of our probe IR pulse after intensity normalization is about 1%. To minimize low-frequency laser fluctuations, the main noise source, every other pump pulse is blocked with a synchronized chopper (New Focus 3500) at 500 Hz, and absorbance change is calculated with two adjacent probe pulses (pump blocked and pump unblocked). The typical noise level in the measured absorbance change is about 0.005 for every pair of pulses. At a 1 kHz repetition rate, the short-term noise is ca. 0.0001 in less than 10 s of data averaging.

Sample Preparation. Nanometer-sized TiO_2 nanoparticles were prepared by the controlled hydrolysis of titanium(IV) tetraisopropoxide.[42] A solution of 5 mL of $Ti[OCH(CH_3)_2]_4$ (Aldrich, 97%) dissolved in 100 mL of isopropyl alcohol was added dropwise (90−120 min) with vigorous stirring to 900 mL of doubly distilled water (2 °C) adjusted to pH 1.5 with HNO_3. (Both titanium(IV) tetraisopropoxide and isopropyl alcohol were purified by distillation before using.) The stirring was continued for 10−12 h until transparent colloids were obtained. The transparent colloids can be stored for over 3 months at low temperature (4 °C) without coagulation. To obtain a powdered sample, 250 mL of the colloidal solution was evaporated (35−40 °C) using a rotary evaporator. The resulting concentrated colloid was dried with an N_2 stream to yield a white powder consisting of nanoparticles with estimated average size of 5 nm.[42] The colloidal samples used in the studies were prepared by dissolving dry TiO_2 powder in N_2-purged D_2O (deuterium oxide) up to a concentration of about 10 g/L. To prepare sensitized nanoparticles, coumarin 343 (C-343), from Aldrich (97%), was added in the TiO_2 colloid and stirred for 2 h. The resulting samples, with a pH of 2.5, were kept under N_2 environment in sealed flow cells. D_2O instead of H_2O solutions were used in the experiments to increase sample transmission in the 5 μm region.

The optical density at 400 nm for the following samples, with 150 μm path length, are shown inside the parentheses: C-343 sensitized TiO_2 in D_2O (∼0.25), unsensitized TiO_2 in D_2O (<0.01), neat D_2O solutions (<0.01), C-343 in dichrolomethane (DCM) (∼0.5), and neat DCM (<0.01). For C-343 sensitized TiO_2 nanoparticle colloid, the absorption at 400 nm is dominated by S_0 to S_1 transition of C-343, and absorption due to TiO_2 nanoparticles is negligible at the experimental concentration. The transient absorption of the excited state of C-343 in the 5 μm region was investigated in DCM rather than D_2O because of the low solubility of C-343 in D_2O. The static FT-IR spectra of C-343 in DCM or adsorbed on TiO_2 show negligible absorbance in the 1800−2200 cm^{-1} region. For all the measurements reported here, the pump wavelength was set at 400 nm and the probe wavelength was tunable from 1850 to 2150 cm^{-1}. For colloid samples, a typical pump pulse with beam diameter of 300 μm and energy of 10 μJ was used. All solution samples were flowed rapidly and continuously to prevent photoproduct buildup. The bulk single rutile TiO_2 crystal (5 mm × 5 mm × 1 mm) used in this study, which has an optical density >2OD at 400 nm, was purchased from Cleveland Crystal. To avoid damaging the crystal, the pump energy was reduced to about 0.3 μJ.

Results

To characterize the IR absorption of electrons in TiO_2 semiconductor, transient IR absorption in a bulk rutile TiO_2 crystal was studied. Electron and hole pairs were created by excitation of the band gap transition resulting in a rise in the IR signal around 5 μm. Shown in Figure 1 are the transient kinetics, measured at 1960 cm^{-1}, of the bulk crystal after 400 nm excitation. The decay of the signal within the first nanosecond is characterized by a pulse width limited decay and a subsequent slow decay of the amplitude by approximately 5% from 1 ps to 1 ns. The decay kinetics at different wavelengths are identical in the 1950−2050 cm^{-1} region. Shown in the insert of Figure 1 is a spectrum of the transient IR signal at 3 ps.

Shown in Figure 2 are transient IR spectra of C-343 sensitized TiO_2 nanoparticle colloidal solution after 400 nm excitation. The open circles, full circles, full triangles, and full diamonds correspond to spectra at 1 ps, 10 ps, 50 ps, and 1 ns, respectively. Shown in Figure 3 are transient IR signals at 2000 cm^{-1} in C-343 sensitized TiO_2 nanoparticles in D_2O (connected full

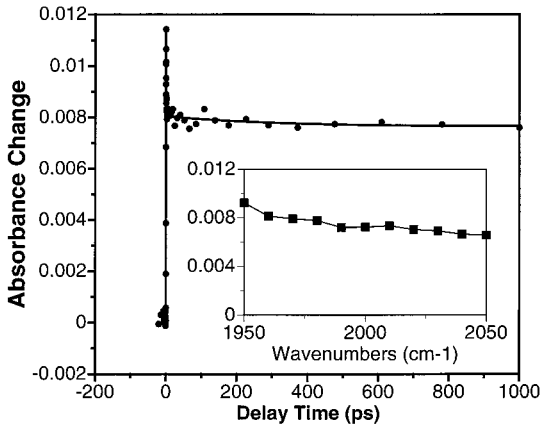

Figure 1. 1. Kinetics of transient IR signal in a bulk TiO_2 crystal after 400 nm excitation measured at 1960 cm^{-1}. Shown in the insert is a transient spectrum at 3 ps.

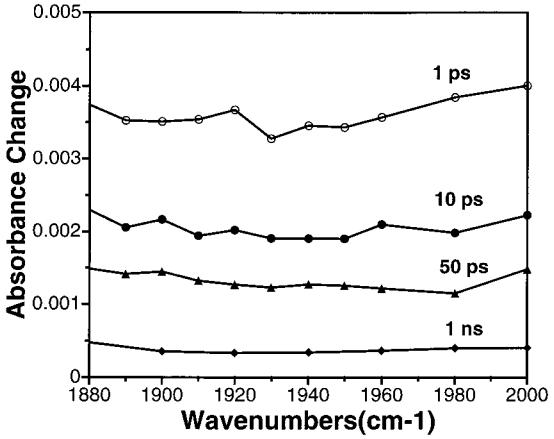

Figure 2. 2. Transient IR spectra of C-343 sensitized TiO_2 nanoparticles in D_2O at 1 ps (open circles), 10 ps (full circles), 50 ps (triangles), and 1 ns (diamonds) after 400 nm excitation.

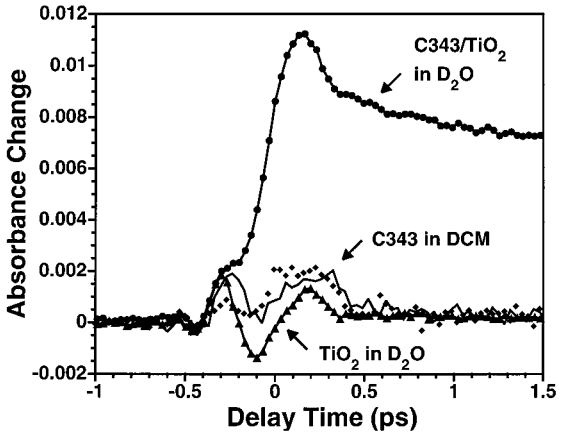

Figure 3. 3. Comparison of transient IR signals measured at 2000 cm^{-1} in samples of C-343 sensitized TiO_2 nanoparticles in D_2O, unsensitized TiO_2 nanoparticles in D_2O, C-343 in DCM, and neat DCM, after 400 nm excitation.

circles), unsensitized TiO_2 colloid in D_2O (connected triangles), C-343 in DCM (diamonds), and neat DCM(solid line) measured under the same pump power at 400 nm. The transient signal from neat D_2O (not shown) is identical to that of the unsensitized TiO_2 colloid in D_2O, suggesting that the observed signals in both samples are due to nonlinear pump−probe interaction in the solvent as a result of the high pump power used in our experiment. These solvent signals are highly reproducible and

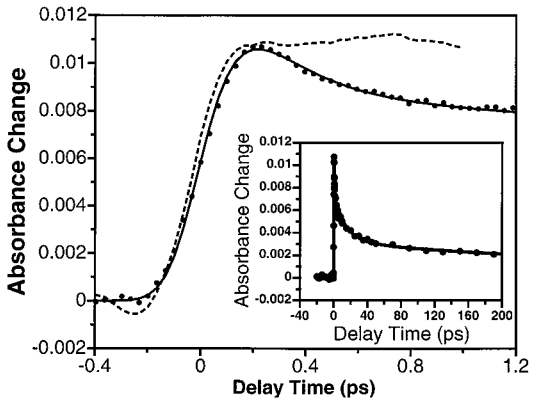

Figure 4. 4. Kinetics for sensitized TiO_2 nanoparticle at 2000 cm^{-1} after subtraction of solvent background signal. Shown in the insert is a kinetics trace in a longer time scale. The experimental data points are represented by full circles, and the best fit with a 135 fs rise time is shown by the solid line. The dash line, which indicates an instantaneous rise, is a kinetics trace measured in a thin silicon wafer.

can be subtracted from the kinetics. The kinetics trace for C-343 sensitized TiO_2 nanoparticles after the subtraction of the corresponding solvent background at 2000 cm^{-1} is shown in Figure 4. Kinetics in a longer time scale (up to 200 ps) are shown in the insert of Figure 4. The rise time of the observed signal can be well fit by convolution of a single-exponential rise and the instrument response function, represented by a Gaussian function with 160 fs fwhm. The instrument response function was obtained by fitting the rise time of the kinetics measured in a thin silicon wafer, which has an instantaneous response, as shown by the dash line in Figure 4, under the same experimental conditions. The solid line in Figure 4 is a fit to the kinetics at 2000 cm^{-1} with a rise time constant of 135 fs. The best fit to the kinetics at 1900, 1950, and 2000 cm^{-1} yields time constants ranging from 100 to 150 fs. We therefore report an average rise time of 125 ± 25 fs. The decay kinetics are also similar in this spectral region and can be well fit by multiple exponential decays with time constants of 0.15, 15, and 300 ps.

Discussions

The band gap energy for the rutile type TiO_2 crystals is around 3.02 eV (or 413 nm).[43] Optical excitation at 400 nm leads to the generation of electrons in the conduction band and holes in the valence band, as indicated by the appearance of the transient IR signal shown in Figure 1. Although the detailed IR absorption spectra of these charge carriers have not been well characterized for undoped TiO_2 crystals, reduced rutile TiO_2 crystals were reported to have significant absorption in the mid-IR region due to excess electrons in the conduction band, which were introduced as a result of reduction.[43] The typical mid-IR absorption spectra of electrons in semiconductor are broad consisting of free carrier absorption, intraband transitions, and trap states.[40] While the observed IR signal shown in the insert of Figure 1 is consistent with the broad IR absorption of electrons, the assignment of the relative contributions of different transitions to the observed signal is not possible due to the very small spectral region studied so far. Future experiments in a much wider spectral range will enable a more detailed analysis. At present, our main goal is to demonstrate the mid-IR absorption of charge carriers in TiO_2 crystals and to compare its general feature with that in nanoparticles. It should be pointed out that the detailed IR spectra of electrons in rutile crystals may be different from those of anatase nanoparticles.

C-343 sensitized TiO_2 nanoparticles have been shown to undergo efficient electron injection from C-343 excited state

to TiO_2 conduction band upon the photoexcitation of C-343.[26,41] Using the fluorescence up-conversion technique, forward electron injection time of 180 ± 50 fs was inferred from the fluorescence decay time of C-343 in a colloidal solution of sensitized TiO_2 nanoparticles in H_2O (with 5% acetone).[26] This reported ultrafast injection time is consistent with a measured high injection quantum yield (>80%) in C-343 sensitized nanocrystalline TiO_2 films.[41] As shown in Figure 2, a broad mid-IR absorption is observed for the C-343 sensitized TiO_2 system after 400 nm excitation. Although this broad absorption feature is a typical signature of electrons in semiconductor, we have also investigated the possible contributions from sources other than injected electrons, such as C-343, D_2O solvent, and unsensitized TiO_2 nanoparticles. As shown in Figure 3, control experiments of C-343 in DCM with 400 nm excitation show only a small transient signal at 2000 cm^{-1}. Since this signal is identical to neat DCM within the signal-to-noise of our experiment, we conclude that the observed signal is due to DCM solvent, and the vibrational spectral changes of C-343 molecules resulting from 400 nm excitation are negligible. It should be pointed out that although C-343 molecules adsorbed on TiO_2 surface are thought to be in the deprotonated form, we expect their transient IR absorption in the 1900−2000 cm^{-1} region to also be negligible, since in the ground state both protonated and deprotonated forms have no noticeable vibrational features in this region. Similarly, 400 nm excitation of unsensitized TiO_2 in D_2O also leads to only a small zigzag type transient signal around $t = 0$ that is identical to neat D_2O solution (not shown here). We therefore conclude that, under our experimental condition, there is no noticeable absorption signal from TiO_2 nanoparticles alone, and the observed signal in the unsensitized colloid can be attributed to nonlinear third-order pump−probe interaction in D_2O solution. Nonlinear signals from neat solvents in a femtosecond visible pump and mid-IR probe experiment have been observed and analyzed,[44,45] and their details will not be discussed here. It is important to note that this nonlinear solvent background signal is very reproducible and can be reliably subtracted from all the kinetics and spectra for the dye sensitized TiO_2 nanoparticles.

For the colloidal solution of C-343/TiO_2, 400 nm excitation leads to a much bigger and longer-lived transient IR signal as shown in Figure 3. Since neither C-343 molecules nor unsensitized TiO_2 nanoparticles have any noticeable transient IR absorption signals under the same experimental conditions, the observed transient IR signal can be attributed to that of injected electrons in TiO_2 plus a small solvent background signal around $t = 0$. After subtracting the background signal, the transient signals that reflect the true contribution of the injected electrons can be obtained. Shown in Figure 4 is the subtracted kinetics trace at 2000 cm^{-1}. Similar kinetics have been obtained in the 1900−2000 cm^{-1} region. The rise time of the transient IR signal represents the formation time of electrons in TiO_2 through injection from the excited state of C-343. The observation of this signal is the most direct evidence of electron injection into the semiconductor. The averaged single-exponential rise time measured in the 1900−2000 cm^{-1} region is 125 ± 25 fs, after deconvolution of the instrument response. Our result is in qualitative agreement with other reported ultrafast injection times of 180 ± 50 fs[26] and less than 20 fs[46] inferred from fluorescence quenching rates in similar systems, although the reasons for the quantitative differences are still unclear. Since femtosecond IR spectroscopy does not rely on the detection of fluorescence, it can be used for sensitizers with weak fluorescence, such as the much studied Ru dye sensitizers. Recently, we applied this technique to the study of Ru N3 sensitized TiO_2 thin films, in which a <100 fs injection time was measured,[47] consistent with reported ultrafast injection times measured in the near-IR and visible region.[20,25] Ongoing studies in our group are systematically examining the dependence of injection rates on the properties of the adsorbates, solvents, and semiconductors.

In addition to injection times, femtosecond IR spectroscopy can also provide information about the subsequent dynamics of the injected electrons within the nanoparticle, such as cooling and trapping, as well as back electron transfer to the sensitizer cations. Unlike bulk crystals, shown in Figure 1, in which the transient signal shows very small decay from 1 ps to 1 ns, the transient signal decays by 10-fold in the same time period in the nanoparticle colloidal solution, as shown in Figures 2 and 4. The best fit to the decay kinetics in the colloid yields multiple exponential decay time constants. The decay of IR absorption can contain dynamics of electron trapping as well as back electron transfer.[22,24,48] Because of the large number of surface defect sites and the small dimension of nanoparticles, the injected electrons are expected to be trapped much more rapidly in nanoparticles than in single bulk crystals.[49] Subpicosecond trapping times of electrons in TiO_2 nanoparticle colloids have been reported by monitoring transient absorptions in the visible region.[50−52] The trapping dynamics can be measured, independent of back ET, by directly creating electrons and holes through the band gap transition in unsensitized nanoparticles. In addition to decaying dynamics, the spectral dependence of the IR signal also contains information about the energetics and mobility of the injected electrons. Transient spectra in a wider range are being measured in sensitized nanoparticle colloids and films. Detailed analysis of the spectra and decay dynamics of injected electrons in TiO_2 nanoparticles will be presented in future publications.

Conclusion

Femtosecond infrared spectroscopy has been used to study interfacial electron transfer between sensitizers and semiconductor nanoparticles. The mid-IR absorption of injected electrons in colloidal TiO_2 nanoparticles have been characterized in the 1900−2000 cm^{-1} region. The direct detection of injected electrons allows unambiguous determination of electron injection processes. For C-343 sensitized TiO_2 nanoparticle colloids in D_2O, the injection time is found to be 125 ± 25 fs, in qualitative agreement with previous reports of ultrafast injection time in similar systems. The subsequent dynamics of the injected electrons have also been measured, yielding multiple exponential decay processes. These decay dynamics are much faster compared with those in a bulk crystal, and the origin of these fast decay processes is still being investigated in our ongoing studies. This study in colloidal solution along with other studies in nanocrystalline thin films[19,47] demonstrates that ultrafast mid-IR spectroscopy is a general and direct tool for studying interfacial electron-transfer processes in sensitized nanoparticle colloids and thin films.

Acknowledgment. The work is supported in part by Petroleum Research Fund, administered by the American Chemical Society, the Emory University Research Committee, and the National Science Foundation CAREER award under Grant No. 9733796. We would like to thank E. W. Castner Jr. at Brookhaven National Laboratory[46] for sharing with us his unpublished results and T. Heimer and E. J. Heilweil at NIST for helpful discussions.

References and Notes

(1) Miller, R. J. D.; McLendon, G. L.; Nozik, A. J.; Schmickler, W.; Willig, F. *Surface Electron Transfer Processes*; VCH Publishers: Weinheim, 1995.

(2) Nozik, A. J.; Memming, R. *J. Phys. Chem.* **1996**, *100*, 13061.

(3) Kamat, P. V. *Prog. React. Kinet.* **1994**, *19*, 277−316.

(4) Oregan, B.; Gratzel, M. *Nature* **1991**, *353*, 737−740.

(5) Marcus, R. A.; Sutin, N. *Biochim. Biophys. Acta* **1985**, *811*, 265.

(6) Newton, M. D.; Sutin, N. *Annu. Rev. Phys. Chem.* **1984**, *35*, 437.

(7) Barbara, P. F.; Meyer, T. J.; Ratner, M. A. *J. Phys. Chem.* **1996**, *100*, 13148−13168.

(8) Marcus, R. A. *J. Chem. Phys.* **1965**, *43*, 679.

(9) Gerischer, H. *Z. Phys. Chem. Frankfurt* **1960**, *26*, 223.

(10) Gerischer, H. *Z. Phys. Chem. Frankfurt* **1961**, *27*, 48.

(11) Levich, V. G.; Dogonadze, R. R. *Dokl. Akad. Nauk SSSR* **1959**, *124*, 123.

(12) Lewis, N. S. *Annu. Rev.Phys. Chem.* **1991**, *42*, 543−80.

(13) Memming, R. *Top. Curr. Chem.* **1994**, *169*, 105.

(14) *Laser Spectroscopy and Photochemistry on Metal Surface, Part I & II*; Dai, H.-L., Wilson, H., Eds.; World Scientific Publishing Co.: Singapore, 1995; Vol. 5.

(15) Eisenthal, K. B. *Chem. Rev.* **1996**, *96*, 1343−1360.

(16) Shen, Y. R. *Solid State Commun.* **1997**, *102*, 221−229.

(17) Richmond, G. L. *Anal. Chem.* **1997**, *69*, A536−A543.

(18) Lanzafame, J. M.; Palese, S.; Wang, D.; Miller, R. J. D.; Muenter, A. A. *J. Phys. Chem.* **1994**, *98*, 11020−11033.

(19) Heimer, T.; Heilweil, E. J. *J. Phys. Chem. B* **1997**, *101*, 10990−10993.

(20) Hannappel, T.; Burfeindt, B.; Storck, W.; Willig, F. *J. Phys. Chem. B* **1997**, *101*, 6799−6802.

(21) Nozik, A. J.; Ellingson, R. J.; Meieer, A.; Kocha, S.; Smith, B. B.; Hanna, M. *Proceedings of the Twenty-first DOE Solar Photochemistry Research Conference*, June 7−11, 1997; p 9.

(22) Martini, I.; Hartland, G. V.; Kamat, P. V. *J. Phys. Chem. B* **1997**, *101*, 4826−4830.

(23) Martini, I.; Hodak, J. H.; Hartland, G. V.; Kamat, P. V. *J. Chem. Phys.* **1997**, *107*, 8064.

(24) Cherepy, N. J.; Smestad, G. P.; Gratzel, M.; Zhang, J. Z. *J. Phys. Chem. B* **1997**, *101*, 9342.

(25) Tachibana, Y.; Moser, J. E.; Gratzel, M.; Klug, D. R.; Durrant, J. R. *J. Phys. Chem.* **1996**, *100*, 20056−20062.

(26) Rehm, J. M.; McLendon, G. L.; Nagasawa, Y.; Yoshihara, K.; Moser, J.; Gratzel, M. *J. Phys. Chem.* **1996**, *100*, 9577−9578.

(27) Lanzafame, J. M.; Miller, R. J. D.; Muenter, A.; Parkinson, B. *J. Phys. Chem.* **1992**, *96*, 2820.

(28) Eichberger, R.; Willig, F. *Chem. Phys.* **1990**, *141*, 159−173.

(29) Lu, H.; Prieskorn, J. N.; Hupp, J. T. *J. Am. Chem. Soc.* **1993**, *115*, 4927−28.

(30) Blackbourn, R. L.; Johnson, C. S.; Hupp, J. T. *J. Am. Chem. Soc.* **1991**, *113*, 1060.

(31) Burfeindt, B.; Hannapel, T.; Storck, W.; Willig, F. *J. Phys. Chem.* **1996**, *100*, 16463.

(32) Liu, D.; Fessenden, R. W.; Hug, G. L.; Kamat, P. V. *J. Phys. Chem. B* **1997**, *101*, 2583−2590.

(33) Murakoshi, K.; Yanagida, S.; Capel, M.; Castner, Jr., E. W. Nanostructured Materials-Clusters, Composites, and Thin Films; *ACS Symp. Ser.* **1997**, *679*, 221..

(34) Liu, D.; Kamat, P. V.; Thomas, K. G.; Thomas, K. J.; Das, S.; George, M. V. *J. Chem. Phys.* **1997**, *106*, 6404.

(35) Fessenden, R. W.; Kamat, P. V. *J. Phys. Chem.* **1995**, *99*, 12902−12906.

(36) Owrutsky, J. C.; Raftery, D.; Hochstrasser, R. M. *Annu. Rev. Phys. Chem.* **1994**, *45*, 519−555 and references within.

(37) Cavicchia, M. A.; Alfano, R. R. *Phys. Rev. B: Condens. Matter* **1995**, *51*, 9629−9633.

(38) Woerner, M.; Elsaesser, T.; Kaiser, W. *Phys. Rev. B* **1992**, *45*, 8378.

(39) Faist, J.; Capasso, F.; Sivco, D. L.; Sirtori, C.; Hutchinson, A. L.; Cho, A. Y. *Science* **1994**, *264*, 553.

(40) Pankove, J. I. *Optical Processes in Semiconductors*; Dover: New York, 1975.

(41) Enea, O.; Moser, J.; Gratzel, M. *J. Electroanal. Chem.* **1989**, *259*, 59.

(42) Bahnemann, D.; Henglein, A.; Lilie, J.; Spanhel, L. *J. Phys. Chem.* **1984**, *88*, 709.

(43) Breckenridge, R. G.; Hosler, W. R. *Phys. Rev.* **1953**, *91*, 793.

(44) Akhremitchev, B.; Wang, C.; Walker, G. G. *Rev. Sci. Instrum.* **1996**, *67*, 3799.

(45) Lian, T. Q.; Kholodenko, Y.; Locke, B.; Hochstrasser, R. M. *J. Phys. Chem.* **1995**, *99*, 7272−7280.

(46) Murakoshi, K.; Yanagida, S.; Castner, Jr., E. W., manuscript in preparation.

(47) (a) Asbury, J. B.; Ghosh, H. N.; Ellingson, R. J.; Ferrere, S.; Nozik, A. J.; Lian, T., accepted for publication in *Ultrafast Phenom.* (b) Ellingson, R. J.; Asbury, J. B.; Ferrere, S.; Ghosh, H. N.; Lian, T.; Nozik, A. J., to be submitted to *J. Phys. Chem. B.*

(48) Moser, J. E.; Gratzel, M. *Chem. Phys.* **1993**, *176*, 493.

(49) Zhang, J. Z. *Acc. Chem. Res.* **1997**, *30*, 423.

(50) Colombo, D. P., Jr.; Bowman, R. M. *J. Phys. Chem.* **1996**, *100*, 18445.

(51) Skinner, D. E.; Colombo, D. P.; Cavaleri, J. J.; Bowman, R. M. *J. Phys. Chem.* **1995**, *99*, 7853−7856.

(52) Colombo, D. P.; Roussel, K. A.; Saeh, J.; Skinner, D. E.; Cavaleri, J. J.; Bowman, R. M. *Chem. Phys. Lett.* **1995**, *232*, 207−214.